Parametric studies for CO_2 reforming of methane in a membrane reactor as a new CO_2 utilization process

Boreum Lee and Hankwon Lim[†]

Department of Advanced Materials and Chemical Engineering, Catholic University of Daegu,
13-13 Hayang-ro, Hayang-eup, Gyeongsan, Gyeongbuk 38430, Korea

Abstract–A one-dimensional reactor model was employed to perform parametric studies for CO_2 reforming of methane in a membrane reactor to investigate its feasibility as a new CO_2 utilization process. The effect of key variables such as hydrogen permeance and Ar sweep gas flow rate to facilitate H_2 transport from a shell side (retentate) to a tube side (permeate) on the performance in a membrane reactor was studied at various temperatures with numerical simulation validated by experimental results. In addition, increase in CH_4 conversion and H_2 yield enhancement observed in membrane reactor was successfully confirmed by profiles of H_2 partial pressure difference between shell and tube sides. From the numerical simulation studies, the feasibility of using a membrane reactor for CO_2 reforming of methane was confirmed by increased CH_4 conversion and H_2 yield enhancement compared to a packed-bed reactor at the same condition, which in turn leads to significant cost reductions due to a reduced operating temperature. Moreover, a window of H_2 permeance and a guideline for Ar sweep gas flow rate for the efficient membrane reactor design was obtained from this study.

Keywords: CO_2 Utilization, CO_2 Reforming, Membrane Reactor, Hydrogen Permeance, Numerical Simulation

INTRODUCTION

Reforming reactions with hydrocarbons have been extensively used for the production of a synthesis gas (syngas), an important precursor for various chemicals such as methanol, alkanes, polyethylene, and ethylene glycols [1-3] and hydrogen, a widely used chemical in petrochemical, chemical, and fuel cell sectors. Coupled with high demand for hydrogen and syngas production, a membrane reactor (MR) combining a reactor and a separator together [4] has been applied to various hydrocarbon reforming reactions [5-19] and even water gas shift reaction [20-30] to obtain various advantages over conventional reactors like improved reactant conversions, product yields, and reduced operating costs caused by better performance compared to conventional reactors, to name a few. Due to the technical and economic challenges related to the sequestration of captured CO_2, methane dry reforming [31,32], a reaction to convert CH_4 and CO_2 into hydrogen or syngas, has gained extensive attention as a practical utilization of CO_2 captured in various industrial sectors. Various research groups reported their results with regard to the incorporation of a membrane reactor concept into methane dry reforming and confirmed improved reactant conversion and hydrogen yield [33-40]. However, their studies mainly focused on the improved reactant conversion and hydrogen yield with a limited range of reaction conditions and membrane properties. Moreover, even though many works have focused on studies for CO_2 reforming of methane in a conventional packed-bed reactor, to our knowledge, little attention has been paid to parametric studies for the effect of a wide range of operating variables and membrane properties on the performance in a membrane reactor from which a practical guideline for an optimized design in a membrane reactor can be sought. In this paper we have investigated the effect of key parameters such as hydrogen permeance, Ar sweep gas flow rate, and operating temperature on the performance in a membrane reactor in terms of CH_4 conversion and H_2 yield enhancement with correlations of H_2 partial pressure difference between shell and tube sides ($P_{H2,\,shell}$-$P_{H2,\,tube}$) in a membrane reactor. From these studies, useful guidelines for the efficient design of a membrane reactor are also presented.

METHODS

1. Model Validation

A one-dimensional reactor modeling, focusing on only single spatial axis, used in the previous studies [30,41-43] has been employed for this study and details are described in Appendix A. The isothermal one-dimension reactor modeling uses differential equations for molar flow rate of each species and incorporates them into reaction rates. Even though only axial direction is considered in this 1-D modeling, it is sufficient enough to provide a preliminary insight to analyze various reactors of interest before fully implementing thorough analysis for concentration and temperature gradients inside reactors. For kinetics used in the modeling, the one proposed by Richardson and Paripatyadar [44] using a Rh/Al$_2$O$_3$ catalyst was used as shown in Eqs. (1), (2), (3), and (4).

[†]To whom correspondence should be addressed.
E-mail: hklim@cu.ac.kr
[‡]This article is dedicated to Prof. Sung Hyun Kim on the occasion of his retirement from Korea University.

The main reactions are CO_2 reforming of methane (Eq. (1)) and reverse water gas shift reaction (Eq. (3)), and the corresponding reaction rate expressions in Langmuir-Hinshelwood type were experimentally obtained at atmospheric pressure using a tubular reactor. Numerical simulation studies were performed with assumptions of (a) steady-state operation, (b) negligible heat transfer, (c) negligible radial concentration gradients, and (d) constant hydrogen permeance along the reactor length.

$$CH_4 + CO_2 \rightarrow 2CO + 2H_2 \tag{1}$$

$$r_1 = k_1 * \left[\frac{K_{CO_2} K_{CH_4} P_{CO_2} P_{CH_4}}{(1 + K_{CO_2} P_{CO_2} + K_{CH_4} P_{CH_4})} \right] * \left[1 - \frac{(P_{CO} P_{H_2})^2}{K_1 P_{CH_4} P_{CO_2}} \right] \tag{2}$$

$$CO_2 + H_2 \rightarrow CO + H_2O \tag{3}$$

$$r_2 = K_2 P_{CO_2} \left[1 - \frac{P_{CO} P_{H_2O}}{K_2 P_{CO_2} P_{H_2}} \right] \tag{4}$$

To reflect pressure difference along the reactor in the modeling, Ergun equation [45] as shown in Eqs. (5), (6) and (7) was used in this study.

$$G = \rho \nu \tag{5}$$

$$\beta_o = \frac{G(1-\phi)}{\rho_o g_c D_p \phi^3} \left[\frac{150(1-\phi)\mu}{D_p} + 1.75G \right] \tag{6}$$

$$\alpha = \frac{2\beta_o}{A_c \rho_c (1-\phi) P_o} \tag{7}$$

To validate the one-dimensional model proposed in this study, we compared numerical results obtained from the modeling to experimental ones obtained from Prabhu et al. [34] at the same reaction conditions. As shown in Fig. 1, numerical results matched well with experimental ones with only slight deviations confirming the validation of our proposed model, and the one-dimensional model was used to carry out parametric studies for key variables, such as hydrogen permeance, Ar sweep gas flow rate, and operating temperature on the performance in a membrane reactor.

2. Reaction Conditions and Membrane Properties in a Membrane Reactor

The reaction conditions and physical properties of a membrane
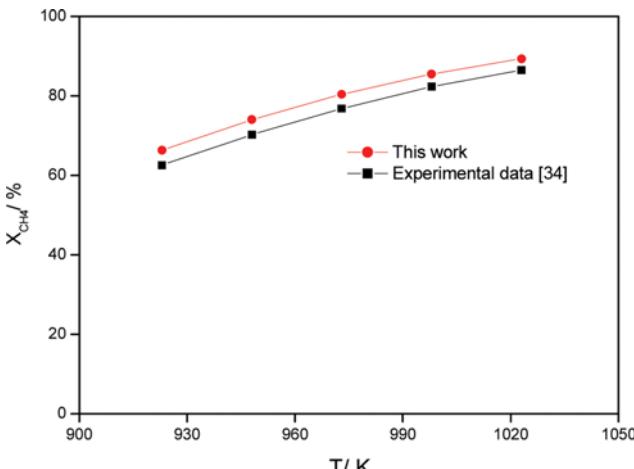
Fig. 1. Model validation with experimental data.

Table 1. Reaction conditions and membrane properties in a membrane reactor

Reactant	$CH_{4\,in}$ (mol s^{-1})	2.4×10^{-5}
	$CH_4 : CO_2$	$1 : 1$
Membrane reactor	T (K)	923-1023
	Catalyst used (g)	3.4
	Catalyst diameter (cm)	0.32
	Void fraction	0.445
	GHSV* (h^{-1})	1138
H_2 separation membrane	Length (cm)	4.5
	Tube diameter (cm)	1.27
	H_2 permeance (mol m^{-2} s^{-1} Pa^{-1})	1×10^{-9}-2×10^{-5}
	H_2 selectivity	10^3

*Gas hourly space velocity

used in this study are presented in Table 1. As a reactant mixture, a stream of CH_4 and CO_2 with a molar ratio of 1 : 1 and Ar as a diluent was fed to a membrane reactor at various operating temperatures from 923 to 1023 K. For a H_2 separation membrane, it was assumed that the membrane length was 4.5 cm with a tube diameter of 1.27 cm to represent a lab-scale study. A wide range of H_2 permeance from 1×10^{-9} to 2×10^{-5} mol m^{-2} s^{-1} Pa^{-1} was employed for this study to represent different types of inorganic and metallic membranes.

RESULTS AND DISCUSSION

1. Effect of H_2 Permeance and Ar Sweep Gas on CH_4 Conversion in a Membrane Reactor

Fig. 2(a) shows the effect of H_2 permeance (1×10^{-9}-2×10^{-5} mol m^{-2} s^{-1} Pa^{-1}) on CH_4 conversion in a membrane reactor at 923 K with a fixed H_2 selectivity of 10^3. The CH_4 conversion in a packed-bed reactor without membrane (dashed line) was found to be 66.28% from the one-dimensional reactor model simulation. Initially, CH_4 conversion in a membrane reactor was similar to one in a packed-bed reactor, but it started to outperform as H_2 permeance increased. Thus, there existed a threshold H_2 permeance from which a membrane reactor outperformed a packed-bed reactor. These results well demonstrate the importance of H_2 permeance as a key factor to derive the extraction of H_2 from a shell side to a tube side in a membrane reactor. However, as H_2 permeance further increased CH_4 conversion reached a plateau for all Ar sweep gas flow rates studied. These phenomena can be explained with further analysis for H_2 partial pressure difference between shell and tube sides, denoted as $P_{H2,\,shell}$-$P_{H2,\,tube}$, as shown in Fig. 2(b). This H_2 partial pressure difference is regarded as a driving force to derive the extraction of H_2 from a shell side to a tube side so that shift of equilibrium to product side can be expected. From Fig. 2(b), it is apparent that the H_2 partial pressure difference reaches zero as H_2 permeance increases, resulting in no further increase in CH_4 conversions in a membrane reactor. From these results, different windows of H_2 permeance for different Ar sweep gas flow rates (narrower window for lower H_2 permeance: for example, 1×10^{-8}-1×10^{-6} mol m^{-2} s^{-1} Pa^{-1} for Ar sweep gas flow rate of 2.7×10^{-5} mol
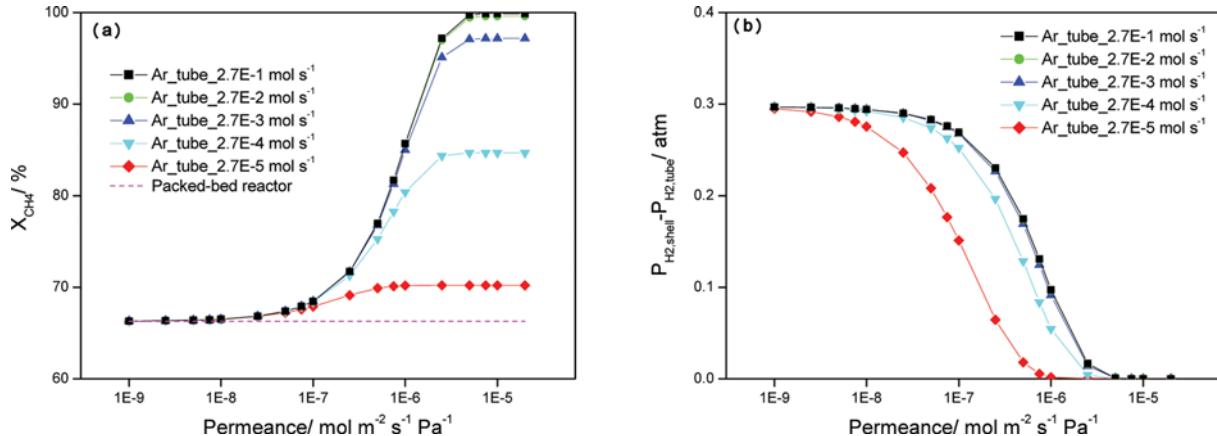
Fig. 2. Effect of permeance on methane conversion (a) and H_2 partial pressure difference (b) with different Ar flow rates at 923 K and H_2 selectivity of 10^3.

s^{-1} and 1×10^{-8}-5×10^{-6} mol m^{-2} s^{-1} Pa^{-1} for Ar sweep gas flow rate of 2.7×10^{-1} mol s^{-1}) can be proposed for the efficient membrane reactor design.

From the studies with Ar sweep gas flow rates, a driving force to derive better sweeping of H_2 from a shell side to a tube side, it was apparent that higher Ar sweep gas flow rate was favorable for the CH_4 conversions in a membrane reactor. With increased Ar sweep gas flow rate in a tube side of a membrane reactor, higher
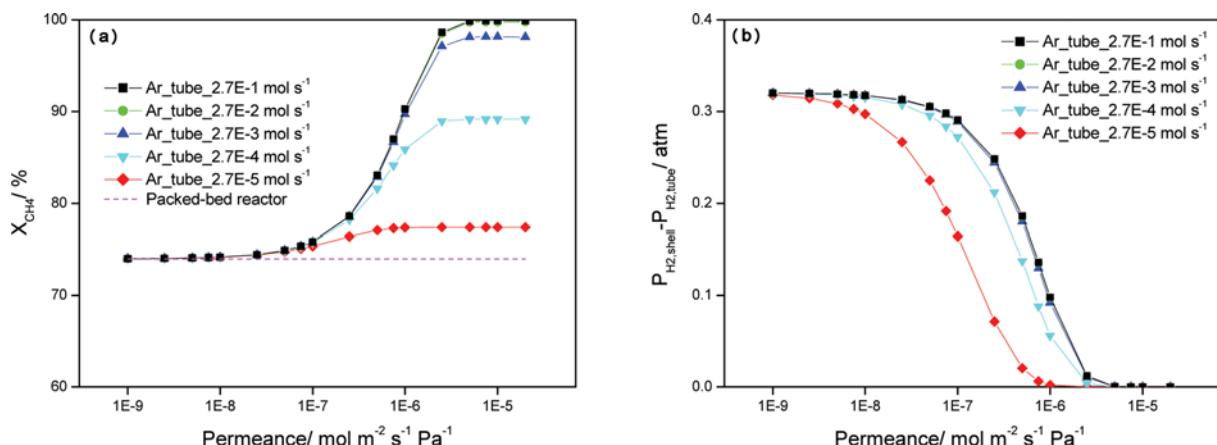

Fig. 3. Effect of permeance on methane conversion (a) and H_2 partial pressure difference (b) with different Ar flow rates at 948 K and H_2 selectivity of 10^3.
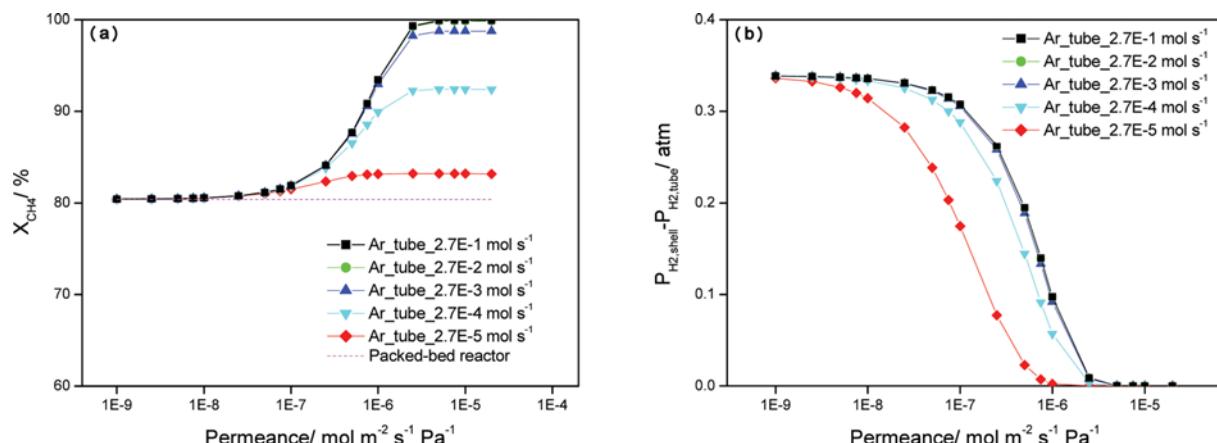

Fig. 4. Effect of permeance on methane conversion (a) and H_2 partial pressure difference (b) with different Ar flow rates at 973 K and H_2 selectivity of 10^3.

H_2 partial pressure difference is clearly shown in Fig. 2(b). At the same time, steeper reduction in H_2 partial pressure difference was observed with lower Ar sweep gas flow rate, and it is surmised that this was attributed to the less increased CH_4 conversion for lower Ar sweep gas flow as shown in Fig. 2(a). Interestingly, similar CH_4 conversions were observed for Ar sweep gas flow rates of 2.7×10^{-2} and 2.7×10^{-1} mol s^{-1} and this can be well explained by the similar H_2 partial pressure difference profiles for two cases.

The same analysis was tried for different temperatures of 948 and 973 K and the results are shown in Fig. 3 and 4, respectively. In

Fig. 3, the dashed line representing CH_4 conversion in a packed-bed reactor of 73.97% at 948 K is shown, and this higher CH_4 conversion compared to one at 923 K (66.28%) is consistent with thermodynamic expectation for an endothermic reaction. For a wide range of H_2 permeance, higher CH_4 conversions than those in a packed-bed reactor were obtained in a membrane reactor after initial thresholds and H_2 permeance was favorable for CH_4 conversions. In addition, Ar sweep gas flow rate was also favorable for CH_4 conversion with no further benefit of Ar sweep gas flow over 2.7×10^{-2} mol s^{-1} again. Less increased CH_4 conversions in a mem-
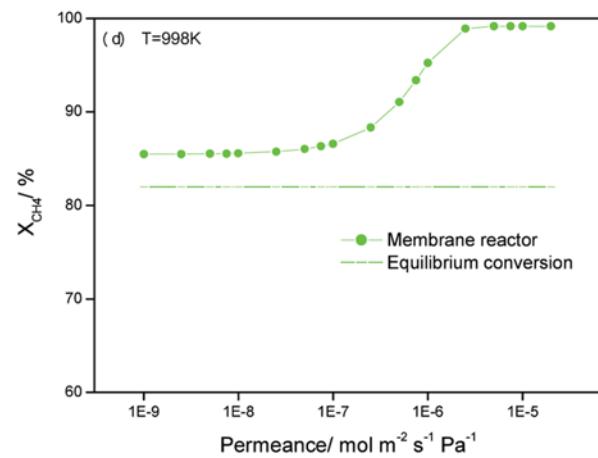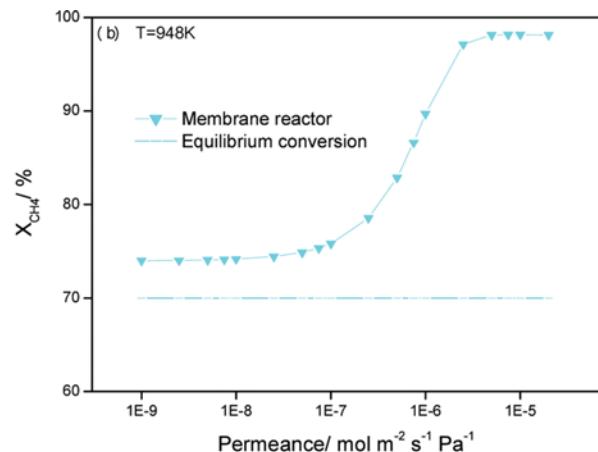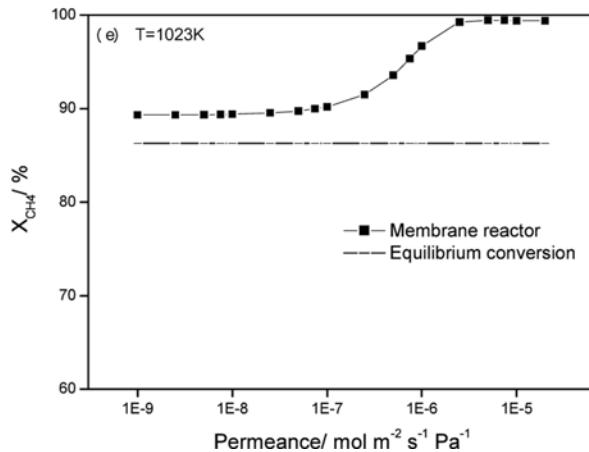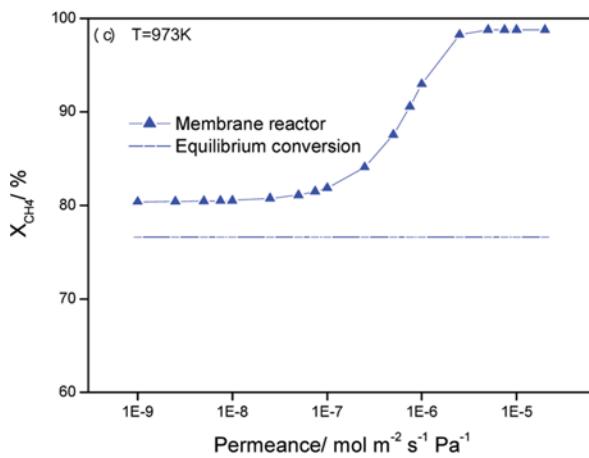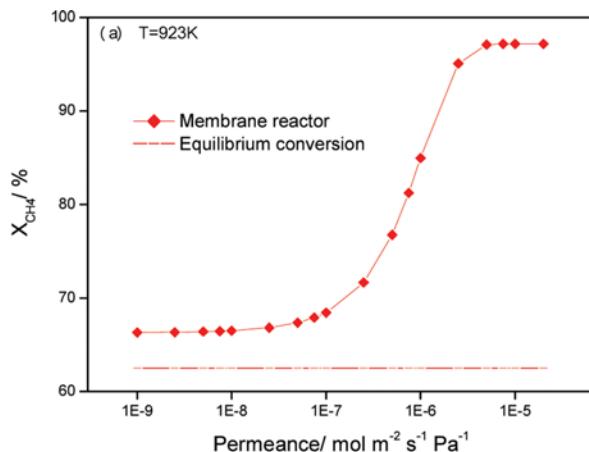

Fig. 5. Effect of permeance on methane conversion at 923-1023 K with an Ar flow rate of 2.7E-3 mol s^{-1} and H_2 selectivity of 10^3.
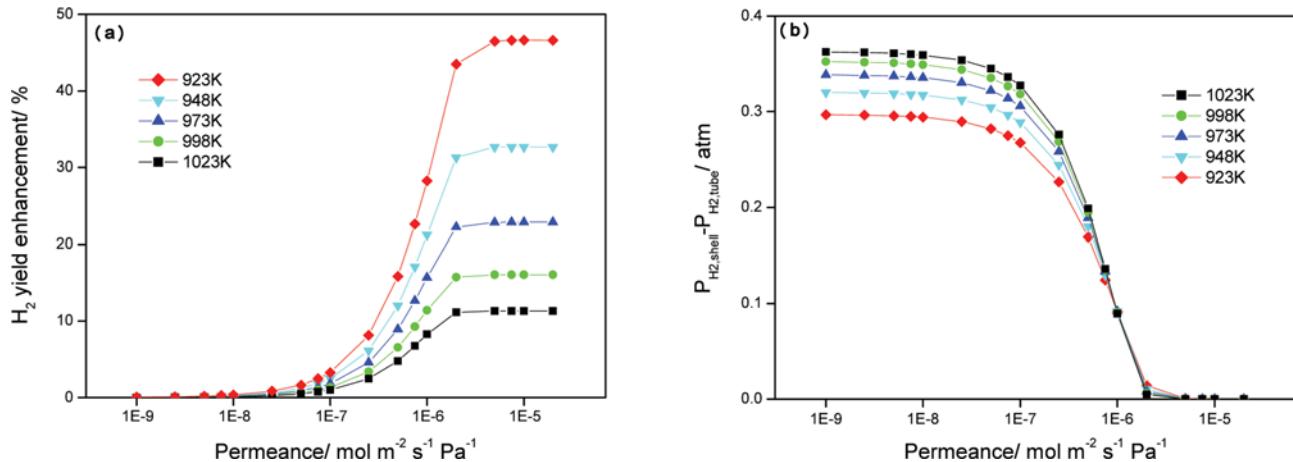
Fig. 6. Effect of permeance on hydrogen yield enhancement (a) and H_2 partial pressure difference (b) at different temperatures with an Ar flow rate of 2.7E-3 mol s^{-1} and H_2 selectivity of 10^3.

brane reactor with lower Ar sweep gas flow rate can be clearly explained by much steeper reduction in the H_2 partial pressure difference in a membrane reactor as shown in Fig. 3(b). Again, there existed a plateau in CH_4 conversion for all cases studied and a window of H_2 permeance similar with 923 K was also observed for the membrane reactor at 948 K.

Fig. 4 shows a CH_4 conversion of 80.39% at 973 K in a packed-bed reactor with a dashed line, and after some initial thresholds higher CH_4 conversions in a membrane reactor was also observed. Two important factors, H_2 permeance and Ar sweep gas flow, were also favorable for increased CH_4 conversion in a membrane reactor, and analysis for H_2 partial pressure difference clearly shows the benefit of using a higher Ar sweep gas flow as a driving force in a membrane reactor. Again, a similar window of H_2 permeance for an efficient membrane reactor design was observed and no further benefit was obtained for Ar sweep gas flow rates over 2.7×10^{-2} mol s^{-1}.

2. Effect of Temperature on CH_4 Conversion and H_2 Yield Enhancement in a Membrane Reactor

To investigate the effect of temperature on CH_4 conversion, numerical simulation was carried out for a membrane reactor at temperatures ranging from 923 to 1023 K with a fixed Ar sweep gas flow rate of 2.7×10^{-3} mol s^{-1} and a H_2 selectivity of 10^3. As shown in Fig. 5, CH_4 conversion increased as H_2 permeance and operating temperature increased. For comparison, equilibrium conversion calculated thermodynamically at each temperature is represented as dashed line [34]. For all conditions studied, better CH_4 conversions were obtained in a membrane reactor compared to equilibrium conversion, substantiating the benefit of the membrane reactor due to shift of equilibrium. Note that the effect of operating temperature on CH_4 conversion was significant at low H_2 permeance, while it was only slight at high H_2 permeance. In addition, it was clearly shown that the effect of H_2 permeance was negligible when H_2 permeance is over about 5×10^{-6} mol m^{-2} s^{-1} Pa^{-1} indicating no further benefit of higher H_2 permeance over this value. From this analysis, it can be concluded that a similar trend of increase in CH_4 conversion with H_2 permeance was observed for all temperatures studied here with significant benefits with lower H_2 permeance.

The effect of H_2 permeance and operating temperature on H_2 yield enhancement, defined as enhanced H_2 yield in a membrane reactor compared to a packed-bed reactor, was studied and a clear trend of higher H_2 yield enhancement with higher H_2 permeance was observed for all temperatures studied, as shown in Fig. 6. As for operating temperatures, higher H_2 yield enhancement was obtained with lower operating temperatures. It was also shown that there existed a H_2 permeance, over which no further increase in H_2 yield enhancement was observed, as supported by H_2 partial pressure difference of zero (Fig. 6(b)). This can work as a useful guideline for optimization of some parameters of membranes used in a membrane reactor.

CONCLUSIONS

A numerical simulation was used for parametric studies for CO_2 reforming of methane in a membrane reactor to investigate its feasibility as a new CO_2 utilization process. A one-dimensional reactor model was employed and successfully validated by previously reported experimental results. Two important parameters, hydrogen permeance and Ar sweep gas flow rate, considered as a driving for H_2 transport through a membrane, were chosen to study the performance in a membrane reactor compared to a packed-bed reactor. It was found from the numerical simulation that both were favorable for CH_4 conversion and H_2 yield enhancement in a membrane reactor. At the same time, CH_4 conversion reached a plateau with increased H_2 permeance and a lower CH_4 conversion was obtained with a lower Ar sweep flow rate, and these results were successfully explained from the analysis for H_2 partial pressure difference between shell and tube sides in a membrane reactor. From the studies with operating temperatures, better CH_4 conversion was obtained in a membrane reactor compared to equilibrium conversion. The effect of operating temperature on CH_4 conversion was significant at low H_2 permeance, while it was only slight at high H_2 permeance, and no further increase in CH_4 conversion was observed for H_2 permeance over about 5×10^{-6} mol m^{-2} s^{-1} Pa^{-1}. Also, higher H_2 yield enhancement was obtained with lower operating temperature, and it reached a plateau as confirmed by

zero H_2 partial pressure difference. The feasibility of using CO_2 reforming of methane as a CO_2 utilization was confirmed from the simulation results, and it was demonstrated that there existed a window of H_2 permeance (for example, 1×10^{-8}-5×10^{-6} mol m^{-2} s^{-1} Pa^{-1} for Ar sweep gas flow rate of 2.7×10^{-1} mol s^{-1}) and a guideline for Ar sweep gas flow rate (no further benefit over 2.7×10^{-2} mol s^{-1}) for efficient membrane reactor design.

ACKNOWLEDGEMENTS

NOMENCLATURE

F_i : molar flow rate of species i on a shell side of a membrane reactor (retentate) [mol s^{-1}]

$F_{i, tube}$: molar flow rate of species i on a tube side of a membrane reactor (permeate) [mol s^{-1}]

W : catalyst weight [g]

k_1 : rate constant of reaction 1 [mol g$_{cat}^{-1}$ s^{-1}]

k_2 : rate constant of reaction 2 (mol atm^{-1} g$_{cat}^{-1}$ s^{-1}]

K_{CO_2} : adsorption equilibrium constant of CO_2 [Pa^{-1}]

K_{CH_4} : adsorption equilibrium constant of CH_4 [Pa^{-1}]

K_1 : equilibrium constant for reaction 1 [Pa^2]

K_2 : equilibrium constant for reaction 2

r_i : reaction rate equation of reaction i [mol s^{-1} g^{-1}]

$r_{i, tube}$: permeation rate equation of species i through a membrane [mol s^{-1} g^{-1}]

$K_{H_2, tube}$: proportional constant of $r_{H_2, tube}$ (mol s^{-1} g^{-1} atm^{-1})

P : total pressure on a shell side of a membrane reactor (retentate) [Pa]

P_o : initial pressure at the entrance condition [Pa]

F_{total} : total molar flow rate on a shell side of a membrane reactor (retentate) [mol s^{-1}]

F_o : initial total molar flow rate at the entrance condition [mol s^{-1}]

P_i : partial pressure of species i on a shell side of a membrane reactor (retentate) [Pa]

P_{tube} : total pressure on a tube side of a membrane reactor (permeate) [Pa]

$F_{total, tube}$: total molar flow rate on a tube side of a MR (permeate) [mol s^{-1}]

$P_{i, tube}$: partial pressure of species i on a tube side of a MR (permeate) [Pa]

$H_{2, permeance}$: hydrogen permeance [mol m^{-2} s^{-1} Pa^{-1}]

F_{CH_4i} : initial molar flow rate of CH_4 [mol s^{-1}]

α_i : hydrogen selectivity of species i

R : gas constant (8.314 J mol^{-1} K^{-1})

T : reactor temperature [K]

ϕ : porosity

g_c : conversion factor [kg m s^{-2} N^{-1}]

D_p : diameter of particle in the bed [m]

μ : viscosity of gas passing through the bed [kg m^{-1} h^{-1}]

υ : superficial velocity [m s^{-1}]

ρ : gas density [kg m^{-3}]

G : superficial mass velocity [kg m^{-2} s^{-1}]

ρ_o : gas density of the fluid at the entrance condition [kg m^{-3}]

ρ_c : density of the solid catalyst particles [kg m^{-3}]

A_c : cross-sectional area [m^2]

REFERENCES

1. J. M. Thomas and W. J. Thomas, *Heterogeneous catalysis,* VCH, Weinheim (1997).
2. M. Seong, M. Shin, J.-H. Cho, Y.-C. Lee, Y.-K. Park and J.-K. Jeon, *Korean J. Chem. Eng.*, **31**, 412 (2014).
3. H.-J. Lee, G. S. Shin and Y.-C. Kim, *Korean J. Chem. Eng.*, **32**, 1267 (2015).
4. J. G. Sanchez Marcano and T. T. Tsotsis, *Catalytic membranes and membrane reactors*, WILEY-VCH, Weinheim (2002).
5. D. Lee, P. Hacarlioglu and S. T. Oyama, *Top. Catal.*, **29**, 45 (2004).
6. S. Irusta, J. Munera, C. Carrara, E. A. Lombardo and L. M. Cornaglia, *Appl. Catal. A: Gen.*, **287**, 147 (2005).
7. T. Tsuru, K. Yamaguchi, T. Yoshioka and M. Asaeda, *AIChE J.*, **50**, 2794 (2004).
8. P. Hacarlioglu, Y. Gu and S. T. Oyama, *J. Nat. Gas Chem.*, **15**, 73 (2006).
9. J. Tong and Y. Matsumura, *Appl. Catal. A: Gen.*, **286**, 226 (2005).
10. C. S. Patil, M. van Sint Annaland and J. A. M. Kuipers, *Chem. Eng. Sci.*, **62**, 2989 (2007).
11. E. Kikuchi, S. Kawabe and M. Matsukata, *J. Jpn. Pet. Inst.*, **46**, 93 (2003).
12. D. Lee, S. Nam, B. Sea, S. Ihm and K. Lee, *Catal. Today*, **118**, 198 (2006).
13. A. Basile, F. Gallucci and L. Paturzo, *Catal. Today*, **104**, 244 (2005).
14. H. Lim, Y. Gu and S. T. Oyama, *J. Membr. Sci.*, **351**, 149 (2010).
15. S. Tosti, A. Basile, F. Borgognoni, V. Capaldo, S. Cordiner, S. Di Cave, F. Gallucci, C. Rizzello, A. Santucci and E. Traversa, *J. Membr. Sci.*, **308**, 250 (2008).
16. S. Vasileiadis, Z. Ziaka and M. Tsimpa, *Int. Trans. J. Eng. Manag. Sci. Technol.*, **2**, 129 (2011).
17. S. Vasileiadis and Z. Ziaka, *Chem. Eng. Sci.*, **59**, 4853 (2004).
18. Z. Ziaka, *Membrane reactors for fuel cells and environmental energy systems*, Xlibris, USA (2009).
19. S. Vasileiadis and Z. Ziaka, *J. Nano Res.*, **12**, 105 (2010).
20. S. Tosti, A. Basile, G. Chiappetta, C. Rizzello and V. Violante, *Chem. Eng. J.*, **93**, 23 (2003).
21. A. Basile, G. Chiappetta, S. Tosti and V. Violante, *Sep. Purif. Technol.*, **25**, 549 (2001).
22. A. Brunetti, G. Barbieri, E. Drioli, K. Lee, B. Sea and D. Lee, *Chem. Eng. Process.*, **46**, 119 (2007).
23. A. Brunetti, A. Caravella, G. Barbieri and E. Drioli, *J. Membr. Sci.*, **306**, 329 (2007).
24. G. Barbieri, A. Brunetti, G. Tricoli and E. Drioli, *J. Power Sources*, **182**, 160 (2008).
25. D. Mendes, V. Chibante, J. Zheng, S. Tosti, F. Borgognoni, A. Mendes and L. M. Madeira, *Int. J. Hydrogen Energy*, **35**, 12596 (2010).
26. D. Mendes, S. Sa, S. Tosti, J. M. Sousa, L. M. Madeira and A. Mendes, *Chem. Eng. Sci.*, **66**, 2356 (2011).
27. Y. Zhang, Z. Wu, Z. Hong, X. Gu and N. Xu, *Chem. Eng. J.*, **197**,

314 (2012).

28. C. A. Cornaglia, S. Tosti, M. Sansovini, J. Munera and E. A. Lombardo, *Appl. Catal. A: Gen.*, **462-463**, 278 (2013).

29. C. A. Cornaglia, M. E. Adrover, J. F. Múnera, M. N. Pedernera, D. O. Borio and E. A. Lombardo, *Int. J. Hydrogen Energy*, **38**, 10485 (2013).

30. H. Lim, *Korean J. Chem. Eng.*, **32**, 1522 (2015).

31. N. Majidian, N. Habibi and M. Rezaei, *Korean J. Chem. Eng.*, **31**, 1162 (2014).

32. N. Rahemi, M. Haghighi, A. A. Babaluo, M. F. Jafari and S. Allahyari, *Korean J. Chem. Eng.*, **31**, 1553 (2014).

33. A. K. Prabhu and S. T. Oyama, *J. Membr. Sci.*, **176**, 233 (2000).

34. A. K. Prabhu, A. Liu, L. G. Lovell and S. T. Oyama, *J. Membr. Sci.*, **177**, 83 (2000).

35. F. Gallucci, S. Tosti and A. Basile, *J. Membr. Sci.*, **317**, 96 (2008).

36. M. L. Bosko, J. F. Munera, E. A. Lombardo and L. M. Cornaglia, *J. Membr. Sci.*, **364**, 17 (2010).

37. J. Li, H. Yoon and E. D. Wachsman, *Int. J. Hydrogen Energy*, **37**, 19125 (2012).

38. F. R. G. Garcia, M. A. Soria, C. Mateos-Pedrero, A. G. Ruiz, I. Rodriguez-Ramos and K. Li, *J. Membr. Sci.*, **435**, 218 (2013).

39. J. Munera, B. Faroldi, E. Frutis, E. Lombardo, L. Cornaglia and S. G. Carrazan, *Appl. Catal. A*, **474**, 114 (2014).

40. S. Sumrunronnasak, S. Tantayanon, S. kiatgamolchai and T. Sukonket, *Int. J. Hydrogen Energy*, **41**, 2621 (2016).

41. S. T. Oyama and H. Lim, *Chem. Eng. J.*, **151**, 351 (2009).

42. H. Lim, *Clean Techol.*, **20**, 425 (2014).

43. A. Alamdari, *J. Nat. Gas Sci. Eng.*, **27**, 934 (2015).

44. J. T. Richardson and S. A. Paripatyadar, *Appl. Catal.*, **61**, 293 (1990).

45. H. S. Fogler, *Essentials of Chemical Reaction Engineering*, Pearson Education, Inc., New Jersey (2010).

APPENDIX A. ONE-DIMENSIONAL REACTOR MODEL

$$\frac{d(F_{CH_4})}{dW} = -r_1 - r_{CH_4, tube}$$

$$\frac{d(F_{CO_2})}{dW} = -r_1 - r_2 - r_{CO_2, tube}$$

$$\frac{d(F_{CO})}{dW} = 2*r_1 + r_2 - r_{CO, tube}$$

$$\frac{d(F_{H_2})}{dW} = 2*r_1 - r_2 - r_{H_2, tube}$$

$$\frac{d(F_{H_2O})}{dW} = r_2 - r_{H_2O, tube}$$

$$\frac{d(F_{i, tube})}{dW} = r_{i, tube}$$

$$\frac{d(P/P_o)}{dW} = -\frac{\alpha}{2y} * \frac{F_{total}}{F_o}$$

$$k_1 = 1290 * \exp\left(\frac{-102065}{RT}\right)$$

$$k_2 = (1.856*10^{-5}) * \exp\left(\frac{-73105}{RT}\right)$$

$$K_{CO_2} = (2.64*10^3) * \exp\left(\frac{37641}{RT}\right)$$

$$K_{CH_4} = (2.63*10^3) * \exp\left(\frac{40684}{RT}\right)$$

$$K_1 = (5.9*10^{14}) * \exp\left(\frac{-258598.7}{RT}\right)$$

$$K_2 = 68.6829 * \exp\left(\frac{-37500.3}{RT}\right)$$

$$P_i = \frac{F_i}{F_{total}} * P$$

$$P_{i, tube} = \frac{F_{i, tube}}{F_{total, tube}} * P_{tube}$$

$$K_{H_2, tube} = \frac{H_{2, permeance} * \text{Membrane Area} * (1.01325*10^5)}{\text{Weight}}$$

$$r_{H_2, tube} = \frac{K_{H_2, tube}}{\alpha_i} * (P_{H_2} - P_{H_2, tube})$$

$$\text{Conversion} = \frac{(F_{CH4i} - F_{CH_4} - F_{CH_4, tube})}{F_{CH4i}}$$